NATURE METHODS

Niche-independent high-purity cultures of Lgr5^{+} intestinal stem cells and their progeny

Xiaolei Yin, Henner F Farin, Johan H van Es, Hans Clevers, Robert Langer & Jeffrey M Karp

Supplementary Figure 1	Cell growth and GFP expression as a function of the culture conditions
Supplementary Figure 2	Single Lgr5-GFP cell culture
Supplementary Figure 3	Colon, stomach and human small intestinal cell culture
Supplementary Figure 4	Differentiation of intestinal stem cells
Supplementary Figure 5	Gene Set Enrichment Analysis (GSEA) of organoids
Supplementary Figure 6	Exploring the mechanism of action for CHIR and VPA
Supplementary Figure 7	Mechanism of VPA
Supplementary Table 1	Summary of growth factors and small molecules used in this study
Supplementary Results	Towards elucidating the mechanism of CHIR and VPA

Nature Methods: doi:10.1038/nmeth.2737

Supplementary Figure 1

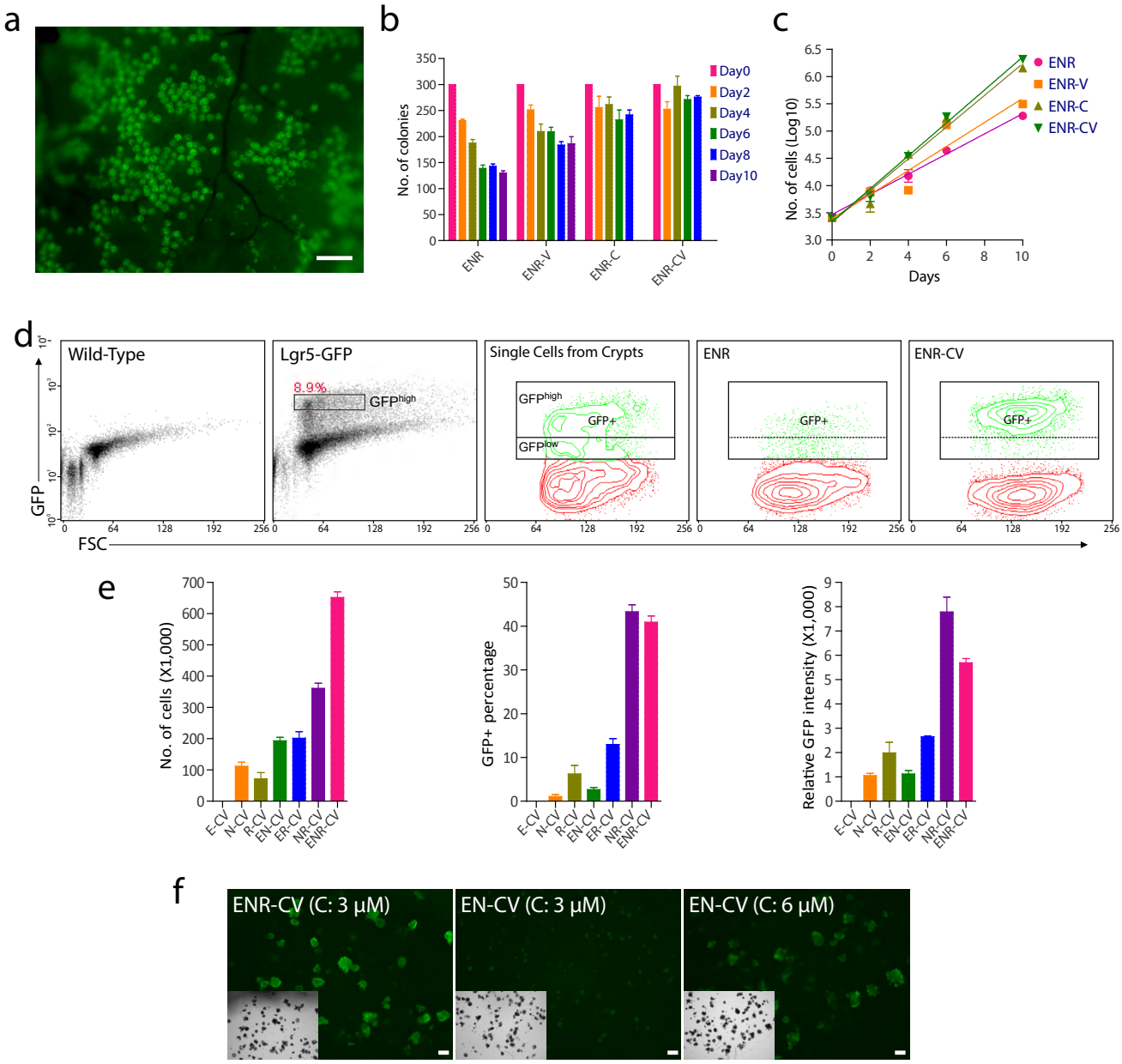

Supplementary Figure 1 | Cell growth and GFP expression as a function of the culture conditions. (**a**) Mosaic expression of Lgr5-GFP *in vivo*. Small intestine was harvested from Lgr5-GFP mice and directly imaged under fluorescence microscopy. While all areas of the small intestine were covered by crypts containing Lgr5^{+} stem cells, approximately half of these crypts contained GFP^{+} cells. (**b**) Colony numbers and (**c**) live single cell numbers from triplicate wells were counted at each time point. Error bars indicate S.D. of triplicate wells. (**d**) FACS sorting of freshly isolated single Lgr5-GFP^{+} cells. GFP^{high} single cell population was collected. Representative FACS analysis showing the gating strategy to define GFP^{+} cell population. Freshly isolated single cells from crypts showed two distinct GFP^{high} and GFP^{low} populations while cultured cells did not show discriminated GFP^{high} and GFP^{low} populations. ENR-CV cultured cells showed a single GFP^{high} population, here all GFP^{+} cells were gated for analysis. Note that the GFP^{-} population includes stem cell that lack GFP reporter expression (i.e. GFP silenced Lgr5+ stem cells). GFP^{neg} cells were largely absent following culture of sorted single Lgr5-GFP (See **Fig. 1d,e**). A total of 10,000 live cells were analyzed for each sample. (**e**) Growth factor requirement for self-renewal of Lgr5^{+} stem cells in the CV culture condition. Crypts were cultured for 6 days in the presence of CHIR and VPA, with EGF, Noggin, R-spondin 1 and their combinations, as indicated. E: EGF (50 ng/ml); N: Noggin (100 ng/ml); R: R-spondin 1 (500 ng/ml); C: CHIR (3 μM); V: VPA (1 mM). Error bars indicate S.D. or triplicate wells. Experiments were performed three times using different animals (n = 3) with similar results. (**f**)Crypts cultured for 6 days in multiple conditions as indicated. GFP and brightfield images are shown.

Nature Methods: doi:10.1038/nmeth.2737

Supplementary Figure 2

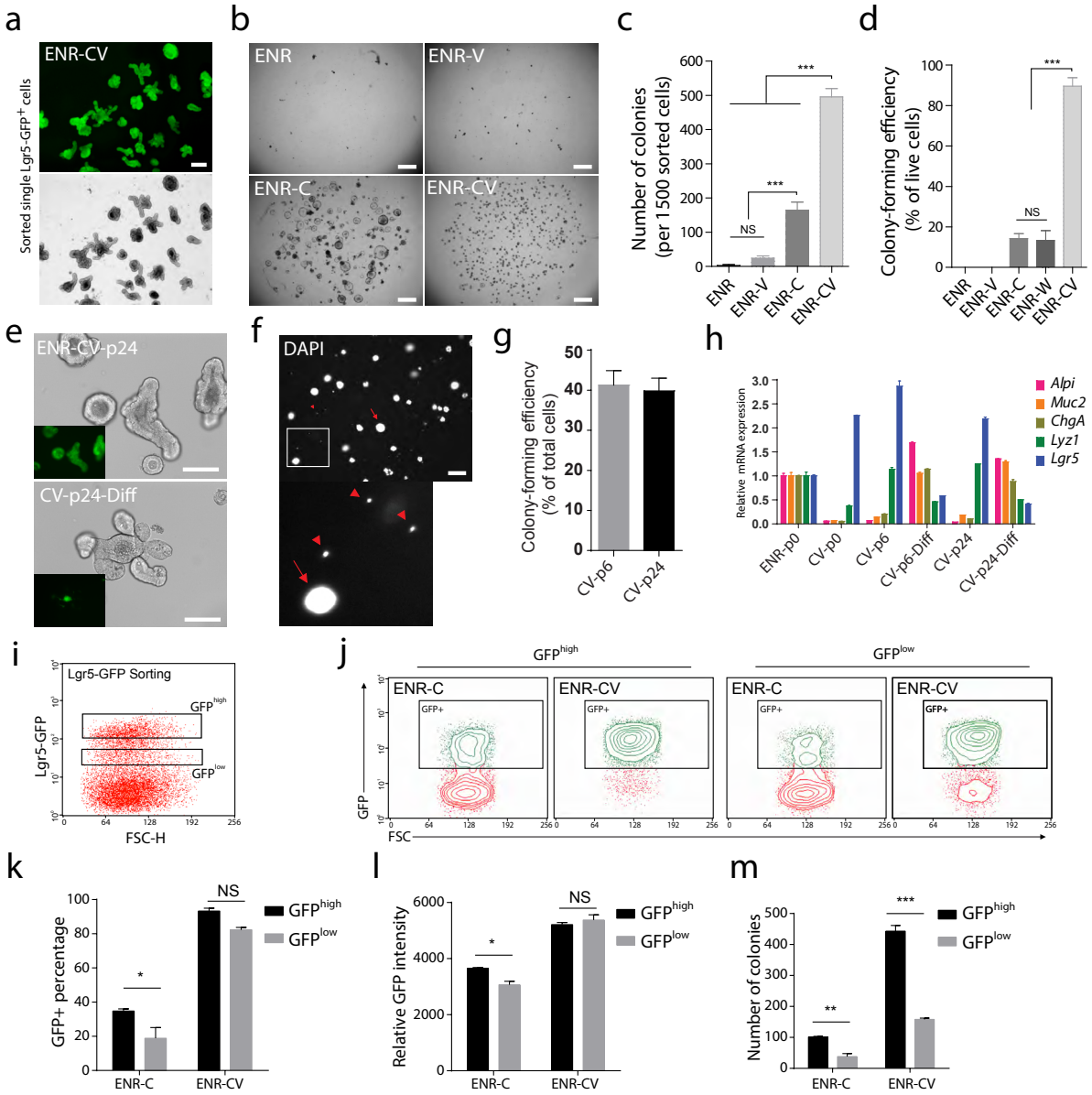

Supplementary Figure 2 | Single Lgr5-GFP cell culture. (**a**) Single isolated Lgr5-GFP^{+} cells cultured for 9 days in CV condition. (**b**) 1500 FACS sorted single Lgr5^{+} cells were cultured in Matrigel under conditions as indicated. Representative images from day 7 cultures are shown and (**c**) quantification of colony numbers. Error bars indicate S.D. of triplicate wells. (**d**) Sorted Single Lgr5^{+} stem cells were seeded in 48-well plates. Viable cell numbers were quantified at 12 h after plating. Colony numbers were counted at day 7 and colony-forming efficiency was quantified based on viable cell numbers. V: VPA; C: CHIR; W: Wnt3a at 100 ng/ml. Error bars indicate S.D. of triplicate wells. Experiments were performed three times using different animals (n = 3) and showed similar results. (**e**) Morphology and GFP images of Lgr5^{+} cells cultured in the CV condition at passage 24 (over 4 months) (top panel), and in spontaneous differentiation condition by transfer CV-p24 cells to ENR condition (bottom panel). (**f**) Representative image showing how colony-forming efficiency of single Lgr5^{+} cells was assessed. The colonies and dead single cells within Matrigel were fixed, air dried (to pellet Matrigel into a single layer) and stained with DAPI. The number of colonies (arrows) and dead cells (arrow heads) were numerated and colony-forming efficiency (CFE) was calculated using: CFE = Number of colonies / (Number of colonies + Number of dead cells). (**g**) Colony-forming efficiency of single Lgr5^{+} cells cultured in the CV condition at passage 6 and passage 24. (**h**) qPCR analysis of Lgr5^{+} cells cultured in the CV condition at passage 0, 6 and 24. CV-p6-Diff and CV-p24-Diff represent spontaneous differentiation conditions by transferring cells from the CV condition to ENR condition. (**i**) FACS sorting of Lgr5-GFP^{high} and GFP^{low} cells. (**j**) FACS analysis of GFP expression of sorted single GFP^{high} and GFP^{low} cells after 9 days in culture, and (**k, l**) quantification of GFP expression. (**m**) Quantification of colony numbers formed by seeding 2,000 single Lgr5^{high} or Lgr5^{low} cells in ENR-C and ENR-CV conditions. In **k–m**, Error bars indicate S.D. of duplicate wells. Scale bars, (**a**) 200 μm, (**e, f**) 100 μm and (**b**) 1 mm. ***P<0.001; **P<0.01; *P<0.05; NS P>0.05.

Nature Methods: doi:10.1038/nmeth.2737

Supplementary Figure 3

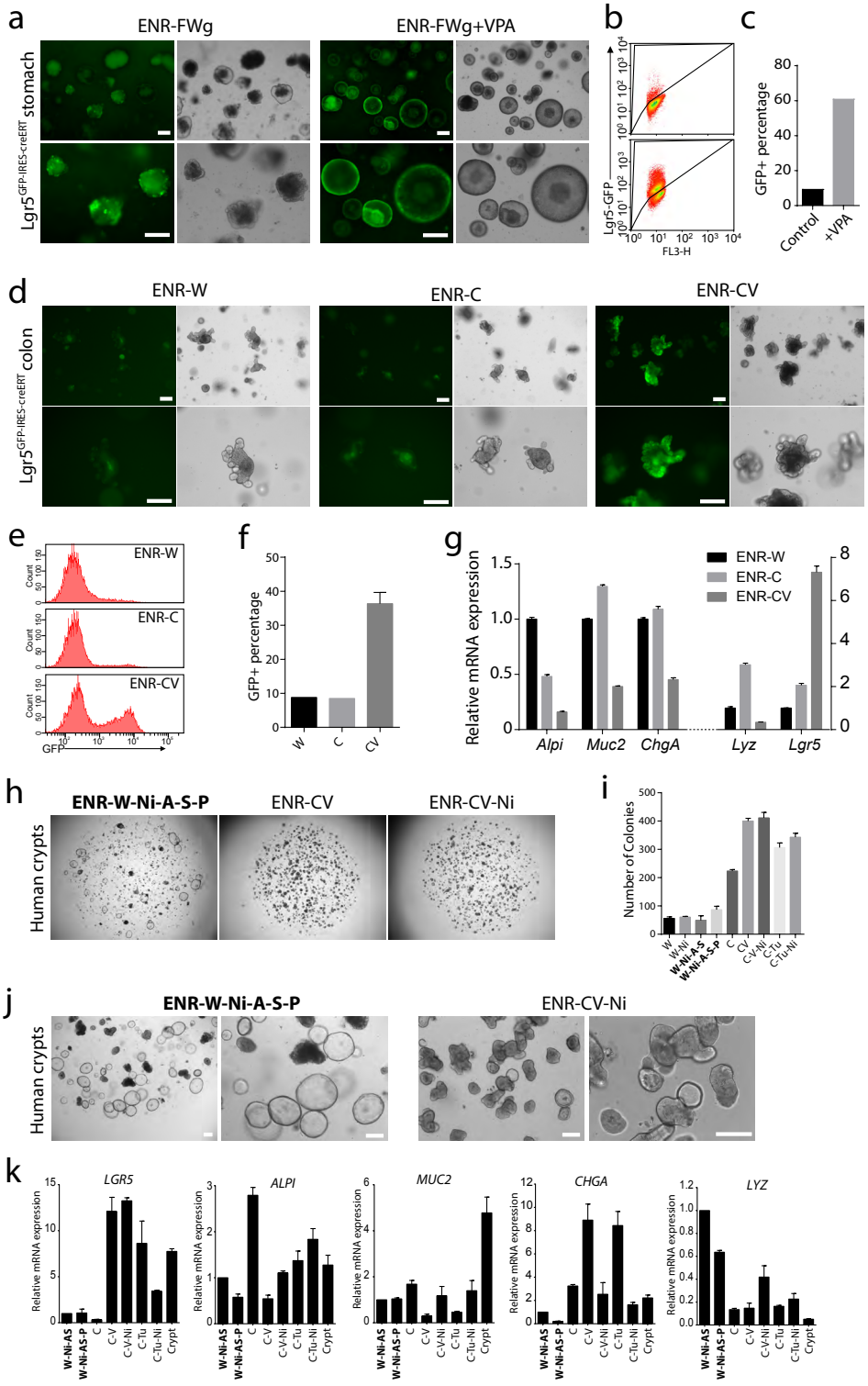

Supplementary Figure 3 | Colon, stomach and human small intestinal cell culture. (**a**) Lgr5-GFP and brightfield images of stomach organoids cultured for 6 days in conditions as indicated. F: FGF10, W: Wnt3a, g: gastrin. (**b, c**) FACS analysis of GFP expression of stomach cultures. (**d**) Lgr5-GFP and brightfield images of colonic organoids cultured for 6 days in conditions as indicated. (**e, f**) FACS analysis of GFP expression of the colonic culture. (**g**) qPCR analysis of marker expression of cultured colonic organoids in multiple conditions. Error bars indicate S.D., n = 3. (**h**) Representative image of freshly isolated human small intestinal crypts cultured in multiple conditions. W: Wnt3a, Ni: Nicotinamide, A: A83-01, S: SB202190, P: PGE2. Titles in bold indicate published culture conditions[1, 2] with gastrin in basal media. (**i**) Quantification of colony numbers. ENR was added in all conditions. Error bars indicate S.D. of triplicate wells. (**j**) Representative image of human small intestinal organoids at passage 2. (**k**) qPCR analysis of marker gene expression of human intestinal crypts cultured in multiple conditions. Error bars indicate S.D., n = 3. All scale bars, 200 µm.

Nature Methods: doi:10.1038/nmeth.2737

Supplementary Figure 4

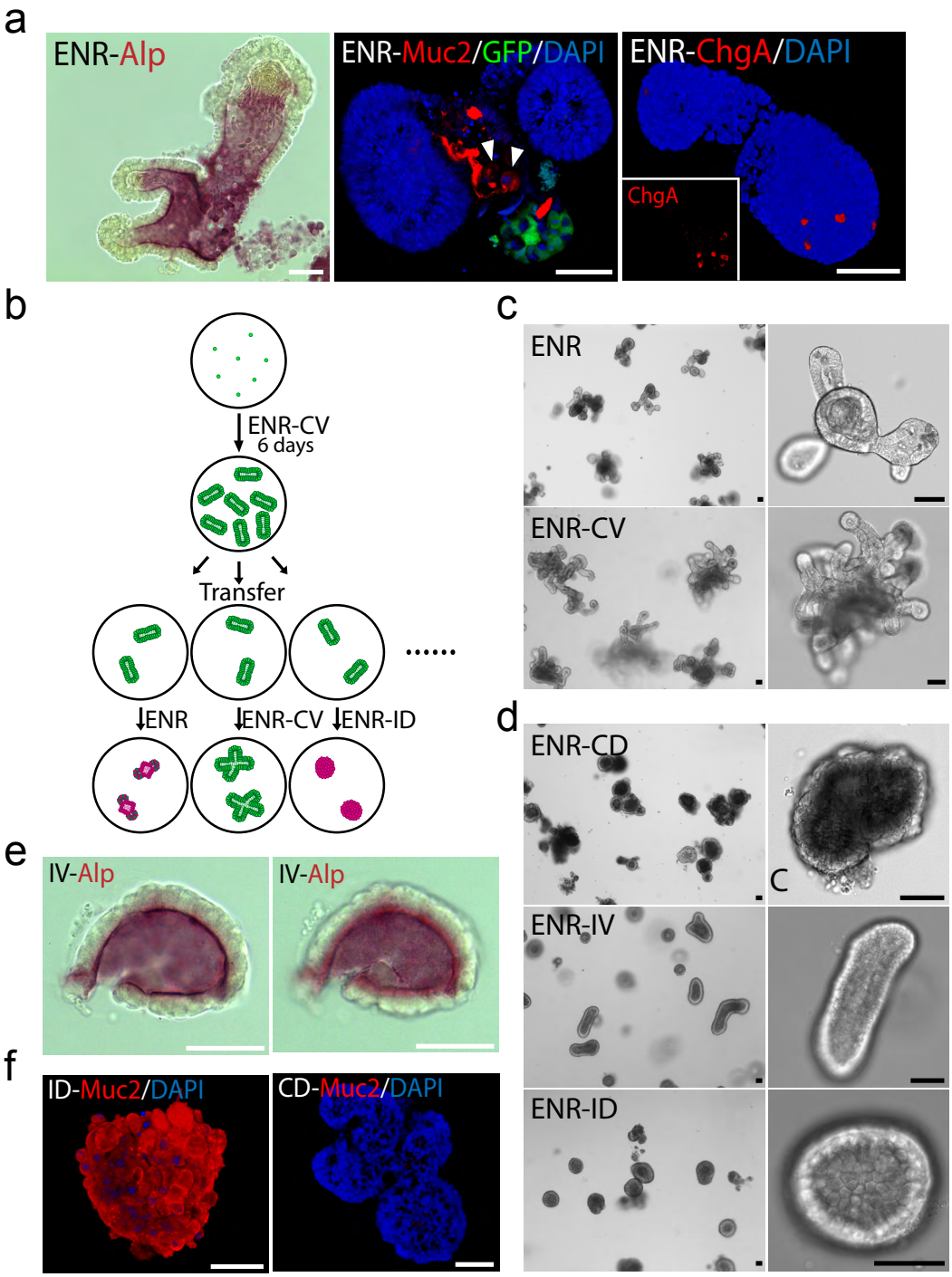

Supplementary Figure 4 | Differentiation of intestinal stem cells. (**a**) Staining of organoids cultured in ENR condition. (left) Alp staining of enterocytes, the organoid was cut open under a dissecting microscope by using a sharp blade and the luminal content was removed before staining. (middle) Muc2 staining of goblet cells (arrows) as well as mucin secreted by goblet cells, and (right) ChgA staining of enteroendocrine cells. GFP^{+} cells indicate Lgr5^{+} stem cells. (**b**) Scheme of differentiation protocol. Single Lgr5^{+} stem cells were cultured in the CV condition for 4–6 days to form colonies. Cell colonies were then harvested, washed, embedded within fresh Matrigel and cultured under multiple conditions. (**c**) Morphology of cell colonies transferred from the CV condition to the ENR condition and cultured for 4 days (upper panels). Colonies continuously cultured in the CV condition are shown as a control (lower panels). (**d**) Morphology of differentiated cells with low and high magnification images for each condition. Note the clear change in morphology for most cells in the CD and ID conditions, which reflects formation of Paneth cells and goblet cells, respectively. (**e**) Alp staining of colonies cultured in IV condition. Apical (left) and homogeneous (right) staining of Alp are shown. (**f**) Muc2 staining of colonies cultured in ID and CD conditions. All scale bars, 50 μm. For images from **c**–**f**, cells cultured in the CV condition at passage number 5 were used.

Nature Methods: doi:10.1038/nmeth.2737

Supplementary Figure 5

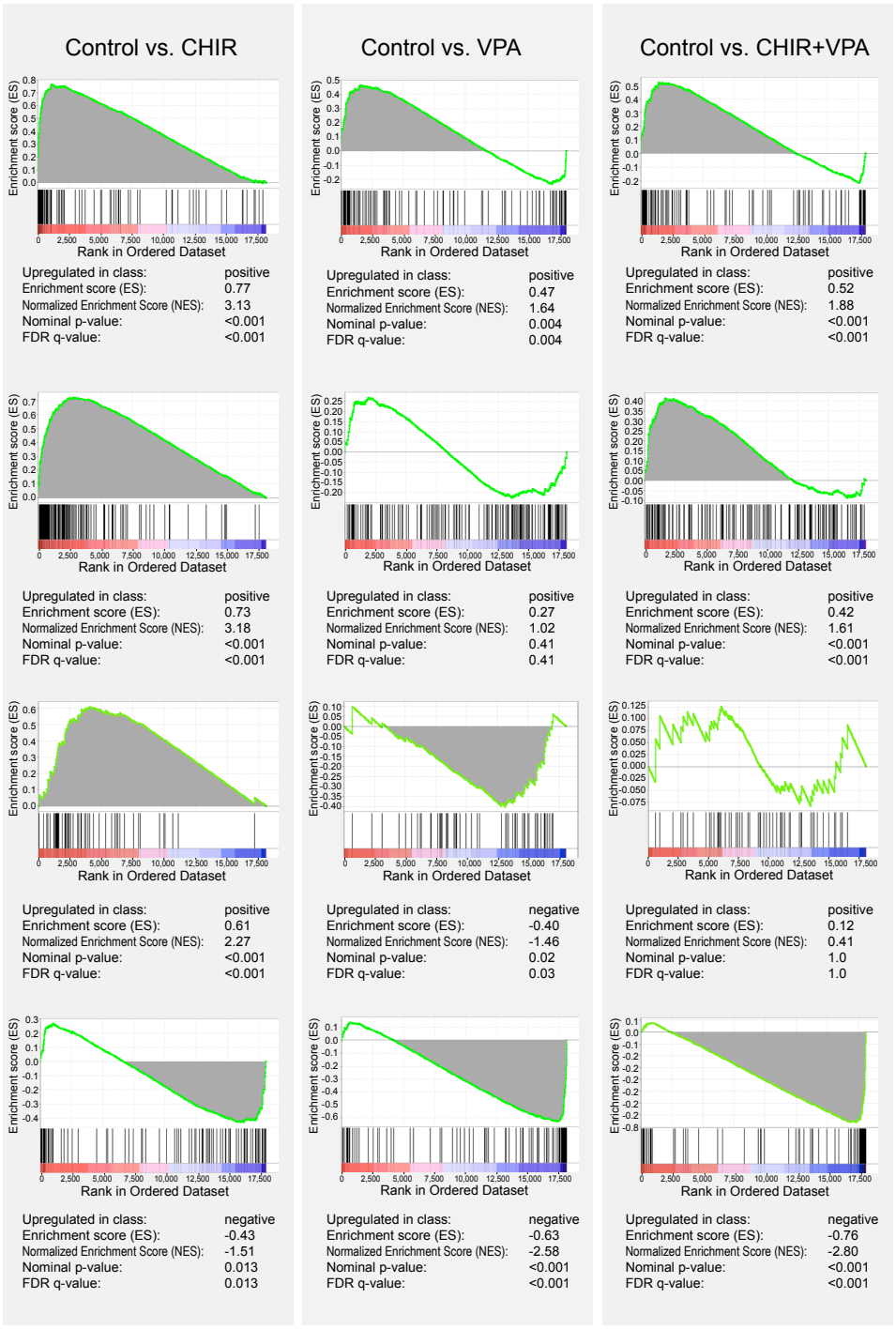

Supplementary Figure 5 | Gene Set Enrichment Analysis (GSEA) of organoids. Ranked gene expression changes (average of duplicate microarray experiments) in (left) organoids (ENR) treated for 6 days with CHIR, (middle) VPA, or (right) CHIR + VPA are shown on the x-axes. Up- and down-regulated genes are indicated with red and blue colors, respectively. Input gene sets were generated from public data sets: 'Stem cell genes' were defined as the 200 most differentially expressed probes in Lgr5-GFP high stem cells (vs. Lgr5-GFP low daughter cells; GEO data set GSE23672) and 'Paneth cells genes' (from sorted Paneth cells vs. Lgr5-GFP stem cells, GSE25109). The 200 most down-regulated probes in organoids 1 day following R-spondin withdrawal (using data set GSE28265) were defined as 'Wnt-target genes'. For analysis of 'proliferation genes' the 44 experimentally verified myc target genes (Yu et al., 2005[3]) were used as input. Position of marker gene sets is indicated with black stripes, the enrichment plot (green line) graphically represents the running enrichment score (ES) for a given gene set. Below the graphs the GSEA output is listed: ES and normalized ES (NES) can be used to compare gene sets of different sizes. The nominal p-value represents the statistical significance of the enrichment score, but is not adjusted for gene set size or multiple hypothesis testing. The FDR q-value (False discovery rate) represents the estimated probability that the normalized enrichment score represents a false positive finding.

Nature Methods: doi:10.1038/nmeth.2737

Supplementary Figure 6

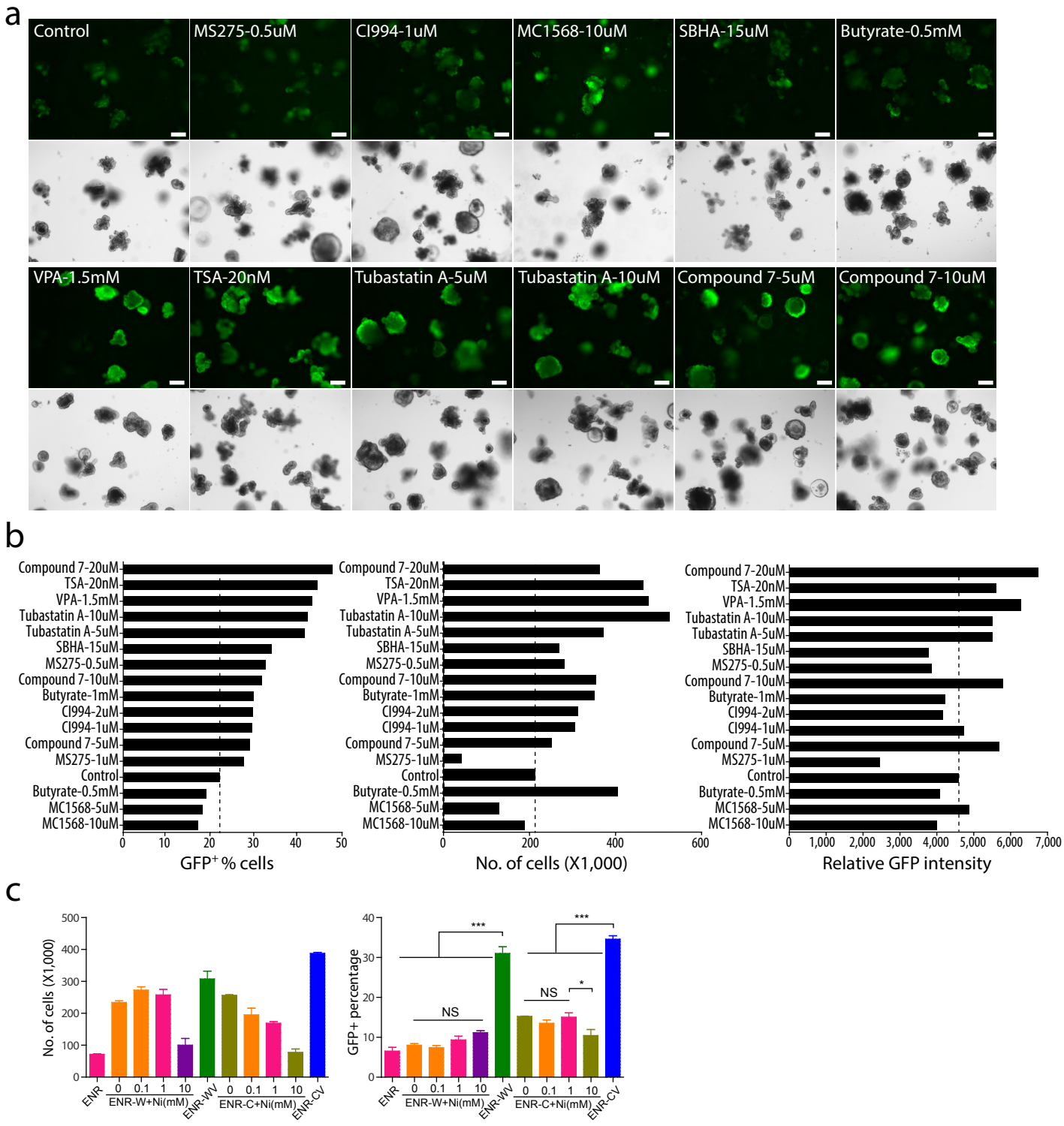

Supplementary Figure 6 | Exploring the mechanism of action for CHIR and VPA. (**a**) 6 day cultures of crypts in ENR-C (Control) condition or together with HDAC inhibitors. (**b**) Quantification of GFP percentage, total live cell number and relative GFP intensity of cells in (**a**). (**c**) The effects of nicotinamide (Ni) in combination with Wnt3a (W, 100 ng/ml) or CHIR (C). Shown are cell numbers and percentage of GFP$^+$ cells of crypts cultured for 6 days in multiple conditions. In all panels, error bars indicate S.D. or triplicate wells. ***P<0.001; **P<0.01; *P<0.05; NS P>0.05.

Nature Methods: doi:10.1038/nmeth.2737

Supplementary Figure 7

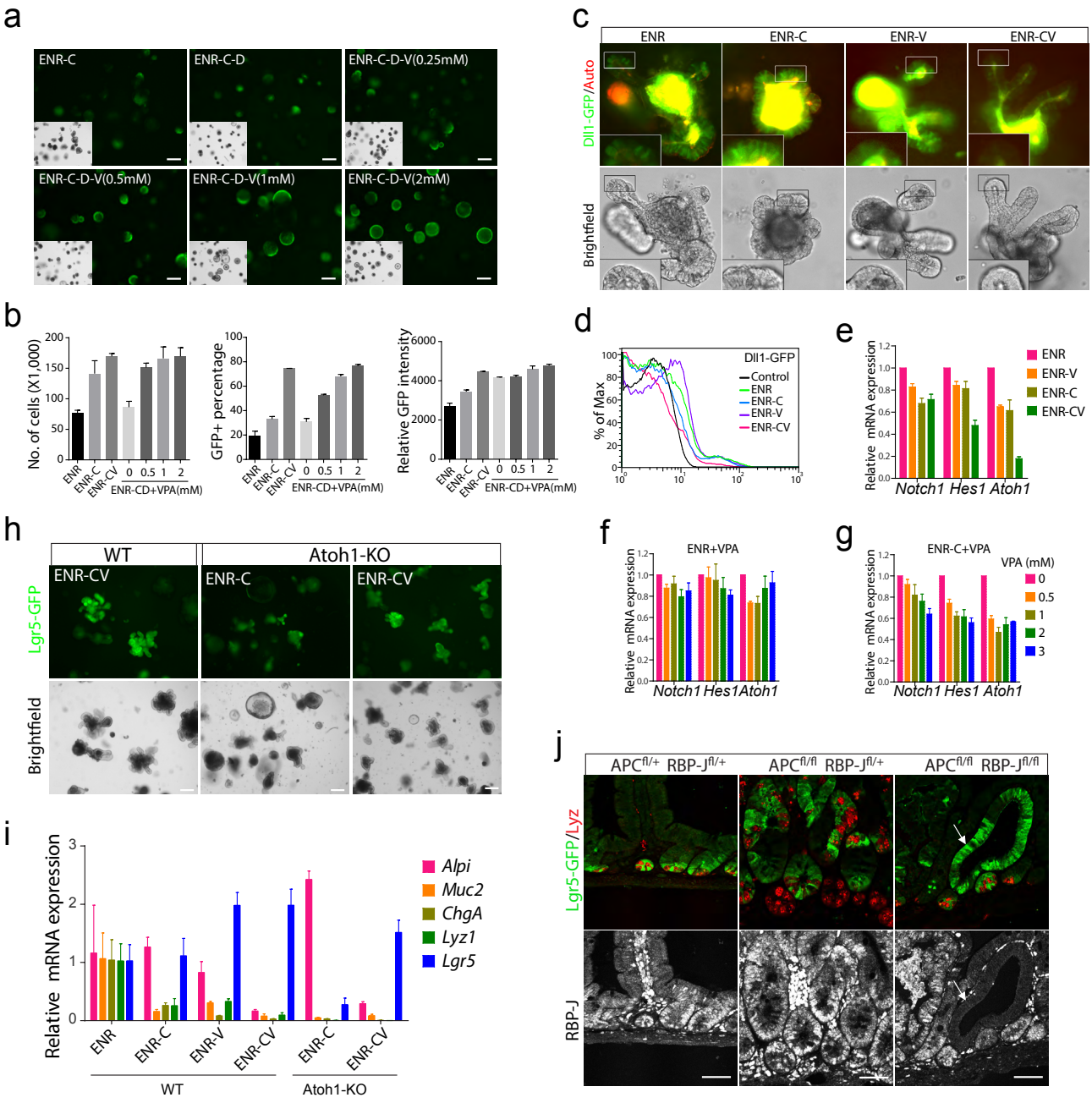

Supplementary Figure 7 | Mechanism of VPA. (**a**) VPA rescues Lgr5-GFP expression following Notch inhibition, titration experiment. Crypts were cultured in ENR-C condition with or without DAPT (D, 5 µM) and varying concentration of VPA (V, 0.25–2 mM) for 3 days. Scale bars, 200 µm. (**b**) Quantification of cell numbers and Lgr5-GFP expression of crypts cultured in ENR-C condition with or without DAPT and varying concentration of VPA (0–2 mM). Error bars indicate S.D. of duplicate wells. (**c**) Intestinal organoids from *Dll1*$^{EGFP\text{-}IRES\text{-}CreERT2/+}$ mice were cultured in multiple conditions for 5 days. Dll1-GFP and brightfield images are shown. Overlay with the red channel shows autofluorescene (yellow signal). (**d**) FACS analysis of Dll1-GFP expression of cells in (**c**). (**f** and **g**) Crypts were cultured in the (**f**) ENR or (**g**) ENR+CHIR conditions for 4 days followed by addition of VPA at different concentrations for another 24 hours. The expression of *Notch1*, *Hes1* and *Atoh1* was analyzed by Real-time RT-PCR. (**h**) Lgr5-GFP expression in wild-type (WT) and Atoh1 knock-out (Atoh1-KO) organoids cultures. (**i**) qPCR analysis of marker gene expression in WT and Atoh1-KO organoids cultured in conditions as indicated. Error bars indicate S.D., n = 3. (**j**) Maintenance of Lgr5-GFP expression in intestinal adenomas lacking RBP-J. Immunfluorescence of paraffin sections 4 weeks following injection of Tamoxifen to induce Cre-activity in *Lgr5-EGFP-ires-CreERT2* mice. (left) Control animal, (middle) homozygous deletion of APC alone and (right) APC/RPB-J deletion are shown. Top panels show GFP staining (Lgr5-reporter, green) and Lysozyme staining (red). Bottom panels show Immunostaining of RBP-J (white) in the same regions. Arrows show that adenomas lacking RBP-J are Lgr5 positive but Lysozyme negative. Scale bars, (**a, h**) 200 µm and (**j**) 50 µm.

Nature Methods: doi:10.1038/nmeth.2737

Supplementary Table 1

Summary of growth factors and small molecules used in this study

Reagent Name	Abbreviation	Final Concentration	Company
EGF	E	50 ng/ml	Invitrogen
Noggin	N	100 ng/ml	Peprotech
R-spondin 1	R	500 ng/ml	R&D
Wnt3a	W	100 ng/ml	Peprotech
CHIR99021	C	3 μM	Stemgent
Valproic Acid	V	1–2 mM	Sigma
IWP-2	I	2 μM	Stemgent
DAPT	D	10 μM	Stemgent
LiCl	Li	5 mM	Sigma
Trichostatin A	TSA	25 nM	Sigma
Suberohydroxamic Acid	SBHA	15 μM	Sigma
Sodium Butyrate	Butyrate	0.5 mM	Sigma
EGF, Noggin, R-spondin 1	ENR	As above	
Nicotinamide	Ni	10 mM	Sigma
gastrin	g	10 nM	Sigma
PGE2	P	0.02 μM	Sigma
A-83-01	A	0.5 μM	Tocris
SB202190	S	10 μM	Tocris
Y-27632	Y	10 μM	Tocris
Tubastatin A		5–10 μM	Chemtek
Compound 7		5–20 μM	Chemtek
MS275		0.5–1 μM	Cayman
CI994		1–2 μM	Cayman
MC1568		5–10 μM	Sigma

Nature Methods: doi:10.1038/nmeth.2737

Supplementary Results

Towards elucidating the mechanism of CHIR and VPA

Besides VPA, TSA, Tubastatin A and Compound 7, we also tested other pan-HDAC inhibitors including SBHA and Butyrate, as well as class I (CI-994, MS275, **Supplementary Fig. 6a,b**), class IIa (MC1568, **Supplementary Fig. 6a,b**) and class III (Nicotinamide, **Supplementary Fig. 6c**) HDAC inhibitors showed no or only moderate effects on GFP expression (**Supplementary Fig. 6a-c**).

Previous reports have shown that Notch pathway activation is required to inhibit secretory cell differentiation and to maintain self-renewal of stem cells[4-8], similar to the effects of VPA. To explore if VPA might target elements of the Notch pathway, we first tested whether Notch inhibition could be rescued by the addition of VPA. Notch/γ-secretase inhibition using DAPT led to impaired cell proliferation and GFP expression, which was rescued by VPA in a dose-dependent manner (**Supplementary Fig. 7a,b**). This suggests VPA acts downstream of Notch-receptor cleavage and could bypass the requirement of ligand-receptor mediated Notch activation. Furthermore, we found that although the addition of VPA alone induced weak global Dll1-GFP expression in *Dll1*$^{EGFP\text{-}IRES\text{-}CreERT2}$ intestinal organoids, VPA+CHIR reduced Dll1-GFP expression (**Supplementary Fig. 7c,d**), which also suggests VPA+CHIR does not function through enhancing Delta-Notch interaction to activate Notch pathway.

VPA has been previously shown to activate Notch1 and Hes1 in cancer cells lines[9, 10] and therefore we tested the effect of VPA on the expression of Notch effectors. We found, however, that addition of VPA moderately decreased the expression of Notch1 and Hes1 in cells cultured for 6 days (**Supplementary Fig. 7e**) or 24 hours (**Supplementary Fig. 7f,g**). Additionally, we observed a pronounced decrease of the negative Notch target Atoh1 (Math1), a transcription factor that is essential for secretory cell differentiation[11, 12]. It has been reported that Atoh1 opposes Hes1 expression[8], constituting a lateral inhibition signaling module that controls the specification of secretory and enterocyte lineages[13]. Intestinal stem cells remain functional both *in vivo* and *in vitro* after Paneth cell ablation induced by Atoh1 deficiency[14, 15], which phenocopies the effects of VPA. We therefore tested whether Atoh1 deficiency mimics the effects of VPA in our system. Indeed, similarly to the effect of VPA, Atoh1 knockout intestinal organoids suppressed secretory marker expression when cultured in the ENR-C condition. Further addition of VPA, however, increased GFP and Lgr5 mRNA expression and downregulated the enterocyte marker Alpi expression compared with CHIR alone, which suggests VPA exhibits other roles in addition to Atoh1 modulation (**Supplementary Fig. 7h,i**).

In the nucleus Notch ON and OFF signals result in activation or repression of effector genes that depend on the transcription factor RBP-J[16]. We then asked whether genetic disruption of both transcriptional programs (i.e. the entire Notch lateral inhibition module) could lead to similar effects as VPA under conditions of high Wnt activation. To test this, we conditionally deleted both RBP-J and the negative Wnt regulator APC in intestinal stem cells by Tamoxifen injection in *Lgr5-EGFP-ires-CreERT2* mice. After 4 weeks the deletion of APC alone caused formation of multiple adenomas[17] that were composed of Lgr5^{+} cells, which were intermingled with Paneth cells. Consistent with a previous report the additional deletion of RBP-J also resulted in adenoma formation[18]. Here, co-immunostaining showed maintenance of Lgr5 expression in the absence of Paneth cells in RBP-J-null adenomas (**Supplementary Fig. 7j**). This result suggests the stem cell marker Lgr5 expression *in vivo* does not rely on the Notch-ON signal when the Notch lateral inhibition module is disrupted, but can be imposed by high Wnt signaling alone.

References:

1. Jung, P. et al. Isolation and in vitro expansion of human colonic stem cells. *Nat Med* **17**, 1225-1227 (2011).
2. Sato, T. et al. Long-term expansion of epithelial organoids from human colon, adenoma, adenocarcinoma, and Barrett's epithelium. *Gastroenterology* **141**, 1762-1772 (2011).
3. Yu, D., Cozma, D., Park, A. & Thomas-Tikhonenko, A. Functional validation of genes implicated in lymphomagenesis: an in vivo selection assay using a Myc-induced B-cell tumor. *Ann N Y Acad Sci* **1059**, 145-159 (2005).
4. Pellegrinet, L. et al. Dll1- and dll4-mediated notch signaling are required for homeostasis of intestinal stem cells. *Gastroenterology* **140**, 1230-1240 e1231-1237 (2011).
5. Milano, J. et al. Modulation of notch processing by gamma-secretase inhibitors causes intestinal goblet cell metaplasia and induction of genes known to specify gut secretory lineage differentiation. *Toxicological sciences : an official journal of the Society of Toxicology* **82**, 341-358 (2004).

Nature Methods: doi:10.1038/nmeth.2737

6. VanDussen, K.L. et al. Notch signaling modulates proliferation and differentiation of intestinal crypt base columnar stem cells. *Development* **139**, 488-497 (2012).
7. van Es, J.H. et al. Notch/gamma-secretase inhibition turns proliferative cells in intestinal crypts and adenomas into goblet cells. *Nature* **435**, 959-963 (2005).
8. Vooijs, M., Liu, Z. & Kopan, R. Notch: architect, landscaper, and guardian of the intestine. *Gastroenterology* **141**, 448-459 (2011).
9. Greenblatt, D.Y. et al. Valproic acid activates notch-1 signaling and regulates the neuroendocrine phenotype in carcinoid cancer cells. *The oncologist* **12**, 942-951 (2007).
10. Stockhausen, M.T., Sjolund, J., Manetopoulos, C. & Axelson, H. Effects of the histone deacetylase inhibitor valproic acid on Notch signalling in human neuroblastoma cells. *Br J Cancer* **92**, 751-759 (2005).
11. van Es, J.H., de Geest, N., van de Born, M., Clevers, H. & Hassan, B.A. Intestinal stem cells lacking the Math1 tumour suppressor are refractory to Notch inhibitors. *Nat Commun* **1**, 1-5 (2010).
12. Yang, Q., Bermingham, N.A., Finegold, M.J. & Zoghbi, H.Y. Requirement of Math1 for secretory cell lineage commitment in the mouse intestine. *Science* **294**, 2155-2158 (2001).
13. van Es, J.H. et al. Dll1+ secretory progenitor cells revert to stem cells upon crypt damage. *Nat Cell Biol* **14**, 1099-1104 (2012).
14. Durand, A. et al. Functional intestinal stem cells after Paneth cell ablation induced by the loss of transcription factor Math1 (Atoh1). *Proc Natl Acad Sci U S A* **109**, 8965-8970 (2012).
15. Kim, T.H., Escudero, S. & Shivdasani, R.A. Intact function of Lgr5 receptor-expressing intestinal stem cells in the absence of Paneth cells. *Proc Natl Acad Sci U S A* **109**, 3932-3937 (2012).
16. Tanigaki, K. & Honjo, T. Two opposing roles of RBP-J in Notch signaling. *Current topics in developmental biology* **92**, 231-252 (2010).
17. Barker, N. et al. Crypt stem cells as the cells-of-origin of intestinal cancer. *Nature* **457**, 608-611 (2009).
18. Peignon, G. et al. Complex interplay between beta-catenin signalling and Notch effectors in intestinal tumorigenesis. *Gut* **60**, 166-176 (2011).

Nature Methods: doi:10.1038/nmeth.2737